

NASA-TM-83020

NASA Technical Memorandum 83020

NASA-TM-83020 19830007881

# Experiments on High Bypass Internal Mixer Nozzle Jet Noise

Jack H. Goodykoontz  
*Lewis Research Center  
Cleveland, Ohio*

December 1982

LIBRARY COPY

JAN 17 1983

LANGLEY RESEARCH CENTER  
LIBRARY, NASA  
HAMPTON, VIRGINIA

**NASA**



# EXPERIMENTS ON HIGH BYPASS INTERNAL MIXER NOZZLE JET NOISE

Jack H. Goodykoontz

National Aeronautics and Space Administration  
Lewis Research Center  
Cleveland, Ohio 44135

## SUMMARY

Model scale jet noise data are presented for a variety of internal lobed mixer nozzle configurations for takeoff power settings in a static environment. The results are presented for a 17.5 cm diameter fan nozzle to show the effect on noise levels caused by changes in geometric shape of the internal, or core flow, nozzle. The geometric variables include the lobe discharge angle, the number of lobes, spacing between the center plug and lobe valley, lobe side wall shape and axial contour of the lobes. An annular plug core flow nozzle was also tested and is used as a baseline for comparative purposes. Comparison of data from the internal lobed configurations showed that the most dominant effect, in terms of the effect on full scale perceived noise levels, was caused by a change in the lobe discharge angle. The results showed that increasing the discharge angle caused an increase as large as 7 dB in sound pressure levels in the high frequency portion of the spectra. Changes in the other geometric variables cause negligible effects.

## INTRODUCTION

Early studies have shown that a decrease in turbofan engine specific fuel consumption at cruise conditions can be obtained by mixing the fan and core flows upstream of the nozzle exit (refs. 1 to 3). As a result of this benefit, with the promise of increased fuel savings, programs to investigate the performance characteristics of different internal mixer nozzle designs have been conducted by the Federal Government and private industry (refs. 4 to 9). The lobed mixer nozzle design (fig. 1) appears to be the most beneficial compared to other mixer designs, in terms of thrust per unit of fuel used (refs. 2 to 4). In addition to the improved performance shown by this design, jet noise suppression benefits have also been reported (refs. 10 to 12). The potential for jet noise suppression was the impetus for the experimental work undertaken and reported herein.

This work is in support of the NASA Energy Efficient Engine (E<sup>3</sup>) program for the development of a fuel efficient high bypass turbofan engine. For such a new engine it is desirable to determine in advance whether or not it is likely to satisfy current noise regulations. Therefore, model scale noise data presented herein were obtained at the Lewis Research Center on a variety of lobed internal mixer nozzle configurations to determine the noise generating characteristics of these designs.

In particular, results are presented to show the effect on noise levels caused by changes in geometric shape of the internal, or core flow, nozzle. The geometric variables include the lobe discharge angle, number of lobes, spacing between the center plug and lobe valley, lobe side wall shape (scal-  
loped, cut-back, corrugated), and axial contour of the lobes. In addition to the lobed configurations, an annular plug core flow nozzle was also tested and is used as a baseline for comparative purposes. The same outer nozzle (shroud or tailpipe) was used for all configurations. Data acquisition was

E-1456

N83-16152#

limited to a range of flow conditions to give subsonic exit Mach numbers and are presented primarily for a typical takeoff power setting. A performance test program was conducted concurrently (not included herein but reported in reference 9) directed toward developing an improved mixer design methodology using a combined analytical and experimental approach. A limited amount of shroud exit plane temperature profile data are presented herein to indicate the degree of mixing.

## APPARATUS AND PROCEDURE

### Facility

A photograph of the flow facility used for the acoustic experiments is shown in figure 2. A common unheated laboratory air source supplied flow for two parallel flow lines, one line for the inner, or core, nozzle and the other for the outer, or fan nozzle. Each flow line had its own air control and flow measuring stations. Mufflers in each line attenuated flow control valve noise. The air for the inner nozzle was heated by a jet engine combustor and combustion noise was attenuated by a second muffler located downstream of the combustor. The air for the outer nozzle was unheated. The large flange upstream of the nozzle exit (fig. 2) was covered with foam rubber to minimize reflections. Also, the nozzle shroud shown in figure 2 was used for the concurrent performance tests and was replaced with a clean design for the noise tests.

Sideline microphone arrays were used for the noise tests. Microphones were placed at a constant 5.0 meters distance from and parallel to the nozzle axis (except for the most rearward microphones), as shown in figure 3(a). The angles ( $\theta$ ) are based on the centerline of the nozzle exit plane. The microphones were located at positions corresponding to multiples of 5 degrees (except for microphones 9 and 18) based on an assumed jet mixing noise distribution. The effective jet noise angles are also indicated in figure 3(a). Both centerline microphones and ground level microphones were used (fig. 3(b)). The centerline array consisted of 0.635 cm condenser microphones with the protective grids removed to improve the microphones' performance at high frequencies. The ground level array consisted of 1.27 cm condenser microphones placed at the equivalent acoustic ray locations as the corresponding centerline microphones, 1.0 cm above grade. A detail of the ground microphone installation is shown in figure 3(c). The ground plane of the test area was composed of asphalt interspersed with patches of concrete.

### Test Nozzles

A schematic of the annular plug core nozzle configuration is shown in figure 4. The shroud, or tailpipe, was common to all configurations and had an exit plane diameter of 17.5 cm. The ratio of fan flow area to core flow area at the core nozzle exit was estimated to be between 2.58 and 2.86 (the smaller ratio was obtained from a comparison of unheated fan and core flow rates at the same pressures, and the higher ratio was determined from design drawings). The axial distance from the inner nozzle exit to the shroud exit, or length of the mixing chamber was about 16.3 cm for all configurations.

A photograph of a typical mixer nozzle configuration is shown in figure 5. Center plugs were contoured to give a constant area distribution through the core passage upstream of the core nozzle exit. Downstream of

the exit all plug contours were the same. Fan to core area ratios (as determined from the ratio of flow rates) varied from 2.40 to 3.50.

The mixer nozzle geometry was varied to investigate differences in mixing effectiveness and performance of the nozzles caused by the variations of mixer geometry (reported in ref. 9). A summary of the variations to the mixer nozzle is shown in figure 6. The variations include the number of lobes, axial contour of the lobes, discharge angle, gap height between the central plug and valley of the mixer nozzle, and side wall modification. The number of lobes (which determines the periphery of the mixer nozzles) ranged from 12 to 24 with the majority of the acoustic data obtained from the 12 lobe configurations. The axial contour determines the amount of turning of the core flow with contour A providing the most turning, contour B the least, and contour C an intermediate case. Configurations with the large discharge angle with contour B (configurations 6, 6C and 6CS) also had an airfoil shaped lobe contour to determine if internal losses could be minimized in this manner. The effect of gap height was compared for two nozzles with the same ratio of fan flow area to core flow area (configurations 3 and 5). Details of the lobe design for configurations 3, 5, and 6 are shown schematically in figure 7 and will be helpful in discussing the acoustic results. It should be noted from the figure that configuration 5 not only has a larger plug gap height, compared to that of configuration 3, but also a smaller lobe discharge angle. Sidewall modification included scalloping and cutting back (physically removing metal from the mixer walls), and corrugating the wall. A photograph of the corrugated wall mixer with the shroud removed, is shown in figure 8.

### Procedure

All tests were conducted with steady-state subsonic flow conditions for specified nozzle total pressures and temperatures. Total pressures and temperatures were measured in low velocity regions upstream of the mixing chamber. Noise measurements were made for equal core and fan stream pressures with pressure ratios (ratio of total pressure to atmospheric pressure) set at a typical takeoff power setting of 1.6. Fan flow was unheated for all tests whereas core flow was heated so that the ratio of core temperature to fan temperature was set and maintained at 2.5. A summary of the flow conditions for the acoustic tests of all configurations is given in table I. Fan and core stream ideal exhaust velocities ( $V_F$  and  $V_C$ ) were calculated by assuming isentropic expansion using the nozzle pressure ratios. The ideal mixed velocity from the shroud exit ( $V_M$ ) was then calculated from the equation shown in the symbol list. As shown in the table, by-pass ratios (ratio of fan flow to core flow) ranged from 3.56 to 5.71 for the configurations tested.

After a steady-state flow condition was attained, an on-line analysis of the noise signal from each microphone in succession was made. One-third octave band sound pressure level spectra were digitally recorded and subsequently processed to give free-field lossless data at the microphone location. To convert to free-field (free from ground reflections) the assumption of a pure harmonic point source and infinite ground impedance was made and ground reflection corrections were calculated for each microphone and frequency (ref. 13). The measured spectral data for each microphone were then adjusted for the ground reflection. Atmospheric attenuation of the noise signal was added to the spectral data to give lossless spectral data (ref. 14). A single spectrum for a given angle (from nozzle inlet) was obtained

by combining the two sets obtained from the ground microphones and centerline microphones. The spectrum from the ground microphones was used over a frequency range from 100 to 1000 Hz and the spectrum from the centerline microphones was used over a frequency range from 5000 Hz to 80 KHz. The data from both microphones were arithmetically averaged over the intermediate frequency range from 1250 to 4000 Hz.

Analysis of the data showed that internal flow noise contaminated the high frequency end of the sound pressure level spectra. Additional testing disclosed that the internal noise originated in the core nozzle feed line. The data presented herein were corrected for internal noise in the following manner. Noise levels were measured with the shroud and core nozzle removed and flow from the core nozzle feed line only, at a rate comparable to that with the nozzle installed. The feed line spectra were then subtracted logarithmically from the mixer nozzle spectra. As a result of this correction, the frequency range over which the data are presented is reduced from the desired maximum value (80 KHz) since the internal noise levels, in some cases, were greater than the mixer nozzle noise levels.

Configurations 1 (fig. 4) and 3, 5, and 6 (fig. 6) were used to obtain total pressure and temperature distributions at the shroud exit for subsonic flow conditions as part of the concurrent performance tests reported in reference 9. Pressure and temperature rakes were positioned at the shroud exit in a plane coincident with the centerline of the lobe (for the mixer configurations) for these measurements. Details of this instrumentation and procedure are given in reference 9.

## AERODYNAMIC RESULTS

Four nozzle configurations were tested to determine radial variation of total pressures and total temperatures at the shroud exit for takeoff power settings. The measurements were made during the concurrent performance tests and are presented herein to indicate, qualitatively, the losses and degree of mixing of the configurations tested and also to explain partially the differences in acoustic characteristics of the nozzles. Mixer nozzle performance results, primarily for cruise conditions, are reported in detail in reference 9.

Pressure profiles for two configurations are shown in figure 9 and are typical of the results for all nozzles tested for these flow conditions. Included in the figure are data for the annular plug core nozzle (configuration 1, fig. 4) and a basic 12 lobe mixer nozzle (configuration 3, fig. 6). The ratio of local total pressure to core (or fan) nozzle total pressure is plotted as a function of radial position in the figure. The ratio of pressures is close to unity (0.96 to 0.98) near midstream and falls off to as low as .92 to .94 near the nozzle centerline and/or shroud wall.

Total temperature variations for all four nozzle configurations are shown in figure 10. The results for nozzles with a nominal by-pass ratio of 3.8 are shown in figure 10(a). Included are results for the annular plug core nozzle and the mixer nozzle with the air foil shaped lobes and large discharge angle (configuration 6). The core flow from the annular plug nozzle undergoes no change in temperature from the measuring station upstream of the core nozzle exit to the exit of the shroud. The mixer nozzle, however, shows a considerable decrease in core temperature from 717 K to a peak temperature of 540 K with the peak displaced radially outward. The shroud peak exit velocity for the configuration with the mixer nozzle is, approximately, 15 percent less than that for the configuration with the annular plug nozzle.

Results are compared for two different mixer nozzle configurations with a by-pass ratio of 5.6 in figure 10(b). The mixer nozzles are essentially the same except for the difference in gap height between the center plug and lobe valley (see fig. 6). For the larger gapped nozzle (configuration 5) the shroud exit temperature near the nozzle centerline is reduced only slightly below that of the core nozzle exit temperature. Reducing gap height (configuration 3) causes the shroud exit temperature to be reduced considerably below that of the core temperature, with the peak temperature displaced radially outward. Peak velocity difference for the two configurations is of the order of 13 percent.

## ACOUSTIC RESULTS

Acoustic data, in terms of sound pressure level spectra at various directivity angles, are presented to show the differences caused by variations to the core nozzle geometry. A comparison of data is made between the annular plug and lobed core nozzle configurations followed by a comparison for variations to the lobed core nozzle. The variations for the lobed core nozzle comparisons are limited to lobe discharge angle and plug gap height. Other variations, such as number of lobes and sidewall treatment showed no appreciable effect on far field noise characteristics. Lobe contour was found to have a minimal effect on the noise characteristics. Finally, a comparison is made between the lobed core nozzle noise characteristics with that for a conical and coaxial-coplanar nozzle.

### Comparison of Lobed Mixer Nozzle Data With Annular Plug Core Nozzle Data

The annular plug core nozzle configuration (configuration 1, fig. 4) incorporates a free mixing process since the fan and core streams are not forcibly mixed upstream of the shroud exit. Aerodynamically, this nozzle serves as a baseline, or least efficient, mixing configuration.

A comparison of the acoustic results for a lobed internal mixer nozzle (configuration 3) and the annular plug core nozzle is shown in figure 11. The data for configuration 3 are also representative of the results that were obtained for configurations 3S and 9, shown in figure 6. Therefore, it is inferred that sidewall scalloping and number of lobes had no appreciable effect on the noise characteristics of internal lobed mixer nozzles.

Spectral characteristics at three different directivity angles are shown in figure 11. At a directivity angle of  $46^\circ$ , figure 11(a), the two nozzles exhibit approximately identical spectral levels and shapes over the frequency range shown. At  $95^\circ$ , figure 11(b), the spectra for the two configurations begin to diverge with the lobed mixer nozzle having smaller low frequency noise levels and larger high frequency levels, with essentially equal peak levels. In the rear quadrant at a directivity angle of  $139^\circ$ , figure 11(c), this trend continues to progress with the lobed mixer nozzle configuration showing considerably smaller low frequency noise levels and lower peak level with larger high frequency levels.

The decreased low frequency noise with the internal lobed mixer nozzle is attributed partly to its lower peak nozzle (shroud) exhaust velocity and partly to the inverted nature of the velocity profile (as implied from the pressure and temperature profile curves of figure 9 and 10, respectively). The increased high frequency noise with the lobed mixer nozzle is believed

to be primarily internal noise caused by fan flow across the outer surfaces of the lobes, as suggested in reference 15, or by core flow scrubbing the interior surface of the shroud nozzle, or by a combination of both. The inverted velocity profile characteristics has been shown to increase high frequency noise levels (ref. 10) and could also be a contributing factor. If the high frequency noise is internally generated it will become a relatively more important contributor to the total noise in a forward flight environment. This is a result of the relative attenuating effects of forward flight on jet mixing noise and internal noise. This was pointed out and substantiated by experimental data in reference 15.

#### Effect of Variation in Lobe Discharge Angle for the Lobed Internal Mixer Nozzle

A comparison of sound pressure levels for two lobed internal mixer nozzle configurations with different lobe discharge angles is shown in figure 12. Data for configurations 3 and 6 are shown in the figure. A direct comparison of the difference in geometry of the two internal nozzles is shown in figure 7. Increasing the lobe discharge angle increases penetration (distance from nozzle centerline to outer extremity of the lobe) and generally increases the mixing effectiveness (ref. 6). Mixing effectiveness was not evaluated for the configurations tested in this program due to the lack of sufficient information. However, the similarity of the temperature profiles for configuration 6 (fig. 10(a)) and 3 (fig. 10(b)) implies that these configurations had approximately the same values of mixing effectiveness. The deviation from the general trend of increasing mixing effectiveness with increase in penetration is possibly a result of flow separation induced by the large flow turning angles occurring in the core nozzle of configuration 6 (ref. 6).

The data for configuration 6 in figure 12 are representative for the results that were obtained for configurations 6CB and 6CS of figure 6 illustrating that sidewall cutback with scalloping has little effect on the noise characteristics of internal lobed mixer nozzles.

As shown in figure 9 and 10 the shroud exit plane pressure and temperature profiles for the two configurations of figure 12 are approximately the same implying that nozzle (shroud) exhaust velocity profiles are approximately the same (at least in a plane downstream of the lobe centerline). Since total flow rate is the same for both configurations (even though by-pass ratios are different) and nozzle exhaust velocities are about the same the two configurations are compared on the basis of the same ideal thrust.

The data in figure 12 indicate that in the forward quadrant at a directivity angle of  $46^\circ$ , figure 12(a), the sound pressure levels are approximately the same over the given frequency range. However, in the rear quadrant at  $95^\circ$ , figure 12(b), and  $139^\circ$ , figure 12(c) the data begin to diverge at about 4000 Hz. At  $139^\circ$ , figure 12(c), the sound pressure levels for the large discharge angle configuration are approximately 7 dB greater at a frequency of 20 kHz. The increase in high frequency noise is speculated to be caused by increased flow impingement on the inner surface of the shroud downstream of the core nozzle exit resulting from the increased lobe discharge angle and increased core mass flow. The increased core flow is an unavoidable circumstance since increasing the lobe discharge angle, while holding other geometric parameters constant, results in larger core area and consequently lower by-pass ratios for a given total flow.

The increase in high frequency noise is detrimental to the perceived noise levels when scaled to full size. For example, extrapolating the model scale data at  $139^\circ$  to full size by a factor of 10 (at a distance of 335 meters and standard day) increased the perceived noise level for the large discharge angle configuration by 4 PNdB over that for the smaller discharge angle configuration. In addition, as mentioned previously, if the increased high frequency noise is internally generated forward flight would have a relatively small attenuating effect on the total noise.

#### Effect of Variation in Mixer Nozzle Plug Gap Height

Acoustic data showing the effect of variation in plug gap height are presented in figure 13 for configurations 3 and 5 (figs. 6 and 7). The two configurations were designed to have the same fan and core stream flow areas at the core nozzle exit plane. As a consequence of this restriction, configuration 5 has a small discharge angle (fig. 7) in addition to having a larger plug gap height (compared to that of configuration 3).

A comparison of the total temperature profiles of figure 10 implies that the velocity profile of configuration 5 more nearly approximates that of the annular plug core nozzle configuration (configuration 1) with the peak velocity occurring on the axis of the nozzle, while configuration 3 exhibits an inverted velocity profile.

The acoustic data of figure 13 show that at a directivity angle of  $46^\circ$ , figure 13(a), the large gap nozzle has slightly larger sound pressure levels for frequencies below 1200 Hz. At higher frequencies the two nozzles have about the same values of sound pressure level. At a directivity angle of  $95^\circ$ , figure 13(b), sound pressure levels for the two nozzles are the same up to 2000 Hz, and then the levels for the large gap nozzles become less.

At  $139^\circ$ , figure 13(c), the large gap nozzle has greater low frequency noise levels and smaller high frequency levels. This trend was similar to that found for the annular plug core nozzle configuration, when compared to configuration 3 (fig. 11). It is assumed that the increased low frequency levels for the large gap configuration is a result of its larger peak nozzle (shroud) exhaust velocity and decreased high frequency levels is a result of the smaller lobe discharge angle and consequent lessening of internal noise generation, along with the elimination of the inverted velocity profile which may contribute to the increased levels of configuration 3 at high frequency.

#### Comparison of Lobed Mixer Nozzle Data With Predicted Conical Nozzle Spectra

A comparison of sound pressure level spectra at different directivity angles for a lobed mixer nozzle (configuration 3) with that predicted for a simple conical nozzle is shown in figure 14. The prediction for the conical nozzle was calculated by the method outlined in reference 16 and includes source position corrections. The comparison was made for the same value of ideal thrust for both nozzles. The conical nozzle exhaust velocity and total temperature was the same value as the mass-weighted values of the mixer nozzle, causing an increase in the area for the conical nozzle of about 35 percent. Also shown on the abscissa in the figure is a second scale that identifies the frequencies and sound pressure level region associated with a full-size engine having a nozzle diameter ten times larger than that of the models (1.75 m for the mixer nozzle shroud and 2.03 m for the conic nozzle).

At a directivity angle of  $46^\circ$ , figure 14(a), the conical nozzle is shown to be louder in the low frequency end of the spectrum up to about 2000 Hz. Above this frequency the two nozzles have the same values of sound pressure level over the limited frequency range shown. At  $95^\circ$ , figure 14(b), the trend is the same except, at this angle, the frequency range over which the conical nozzle dominates is extended to about 4000 Hz. Above 4000 Hz, again the two nozzles have the same sound pressure levels. Farther back in the rear quadrant at  $139^\circ$ , figure 14(c), the conical nozzle still dominates in the low frequency end below 2000 Hz. Above 2000 Hz the conical nozzle sound pressure levels become progressively lower than those of the lobed mixer nozzle. The results at  $139^\circ$  for the conical-mixer comparison are similar (except for levels) to those that were observed for the annular plug-mixer comparison shown in figure 11(c). These observations give further support to the notion that the inverted velocity profile of configuration 3 substantially influences the noise characteristics.

Perceived noise levels calculated for the case shown in figure 14(c) show that the conical nozzle is 3 PNdB quieter than the internal lobed mixer nozzle. This was based on a scale factor of 10, distance of 335 meters, and for a standard day of  $59^\circ$  F and 70 percent relative humidity.

#### Comparison of Lobed Mixer Nozzle Data and Coaxial-Coplanar Nozzle Data

A comparison of internal lobed mixer and coaxial-coplanar noise data is shown in figure 15. The coaxial nozzle data were obtained as part of the work reported in reference 17. The cycle conditions are given in the accompanying table of figure 15 and it should be noted that the cycle conditions for this comparison differ from those for other comparisons reported herein. The ideal thrust for the mixer nozzle configuration (configuration 3) is approximately 9 percent greater than that for the coaxial nozzle so that no attempt was made to alter the data for the slightly different cycle conditions. The total area of the coaxial nozzle is only 1.5 percent greater than that of the mixer nozzle shroud.

At directivity angles of  $46^\circ$ , (fig. 15(a)), and  $95^\circ$ , (fig. 15(b)), the two nozzles have approximately the same values of sound pressure levels over the entire frequency range shown. In the rear quadrant at  $139^\circ$ , figure 15(c), the coaxial nozzle has larger sound pressure levels for the frequencies below 4000 Hz. Above this frequency the levels and trends for the two nozzles are the same. The full scale perceived noise levels (scale factor of 10, 335 meters distance, and standard day) calculated from the data of figure 15(c) shows that the coaxial nozzle is 4 PNdB louder than the mixer nozzle.

#### CONCLUDING REMARKS

The experimental work reported herein indicates that the lobe discharge angle of the core nozzle had the greatest effect on far-field noise characteristics for efficient forced mixer nozzle configurations. The effects of changes in the lobe discharge angle are most noticeable in the rear quadrant near the peak noise location. An increase in high frequency noise was observed, believed to be caused internally by increased scrubbing of the interior surface of the shroud by the core flow, when the discharge angle was increased. The increased high frequency content results in increased values of perceived noise levels at full scale. In addition, when the noise is

generated internally, the total noise reduction would be relatively small in forward flight.

A secondary effect was noticed by increasing the gap between the center plug and lobe valley. In this case, however, increased low frequency noise and decreased high frequency noise were observed near the peak noise location. An examination of the temperature profile at the shroud exit showed this configuration to be an inefficient mixing nozzle.

Changes in other geometric variables such as number of lobes, lobe side wall shape (scalloped, cut-back, corrugated), and axial contour of the lobes caused negligible effects on the noise characteristics.

A comparison of the mixer nozzle spectral data with the spectrum predicted for a conical nozzle showed that, near the peak noise location, the mixer nozzle had smaller values of low frequency sound pressure levels and larger values of high frequency levels. The increased high frequency noise content of the mixer nozzle resulted in a 3 PNdB increase in full scale perceived noise levels for the case considered.

A comparison was also made between mixer nozzle data and coaxial nozzle data at about the same values of ideal thrust. Near the peak noise location the mixer nozzle had smaller values of low frequency sound pressure levels whereas in the high frequency end of the spectrum the levels for the two nozzles were the same. Full scale perceived noise level for the coaxial nozzle was 4 PNdB greater than that for the mixer nozzle.

APPENDIX - SYMBOLS  
(All dimensions in SI units)

A,B,C,	lobe contour defined in figure 6
CB	designates that sidewall of internal lobed mixer nozzle is cutback (see fig. 6)
CS	designates that sidewall of mixer nozzle is cutback and scalloped (see fig. 6)
D <sub>con</sub>	diameter of simple conical nozzle
PR <sub>C</sub>	ratio of core stream total pressure to ambient pressure
PR <sub>F</sub>	ratio of fan stream total pressure to ambient pressure
R <sub>D</sub>	distance from center of nozzle exit plane to microphone location
S	designates that sidewall of intrnal lobed mixer nozzle is scalloped (see fig. 6)
T <sub>C</sub>	core stream total temperature
T <sub>F</sub>	fan stream total temperature
V <sub>C</sub>	core stream ideal velocity calculated by assuming isentropic expansion from core stream pressure to ambient pressure
V <sub>F</sub>	fan stream ideal velocity calculated by assuming isentropic expansion from fan stream pressure to ambient pressure
V <sub>M</sub>	ideal mass weighted mixed velocity defined as $\frac{W_F V_F + W_C V_C}{W_F + W_C}$
W <sub>C</sub>	core stream weight flow
W <sub>F</sub>	fan stream weight flow
Y	distance upstream of nozzle exit plane measured parallel to nozzle axis at microphone sideline locations
θ	directivity angle defined as angle from nozzle inlet

## REFERENCES

1. Pearson, H.: Mixing of Exhaust and By-Pass Flow in a By-Pass Engine. Vol. 66, no. 620, Aug. 1962, pp. 528-530.
2. Frost, T. H.: Practical Bypass Mixing Systems for Fan Jet Aero Engines. Vol. 17, May 1966, pp. 141-160.
3. Hartmann, A.: Studies of Mixing in Ducted Fanjet Engines. NASA TTF-12562, Nov. 1969.
4. Shumper, P. K.: An Experimental Model Investigation of Turbofan Engine Internal Exhaust Gas Mixer Configurations. AIAA Paper 80-0228, Jan. 1980.
5. Povinelli, L. A.; Anderson, B. H.; and Gerstenmaier, W.: Computation of Three-Dimensional Flow in Turbofan Mixers and Comparison with Experimental Data. NASA TM-81410, Jan. 1980.
6. Kuchar, A. P.; and Chamberlin, R.: Scale Model Performance Test Investigation of Exhaust System Mixers for an Energy Efficient Engine (E<sup>3</sup>) Propulsion System. AIAA Paper 80-0229, Jan. 1980.
7. Kozlowski, H.; and Kraft, C: Experimental Evaluation of Exhaust Mixers for an Energy Efficient Engine. AIAA Paper 80-1088, June 1980.
8. Anderson, B.; Povinelli, L.; and Gerstenmaier, W.: Influence of Pressure Driven Secondary Flows on the Behavior of Turbofan Forced Mixers. NASA TM-81541, July 1980.
9. Anderson, B.; and Povinelli, L.: Factors Which Influence the Behavior of Turbofan Forced Mixer Nozzles. NASA TM-81668, Jan. 1981.
10. Crouch, R. W.; Coughlin, C. L.; and Paynter, G. C.: Nozzle Exit Profile Shaping for Jet Noise Reduction. J. Aircr. vol. 14, no. 9, Sept. 1977, pp. 860-867.
11. Packman, A. B.; and Eiler, D. C.: Internal Mixer Investigation for JT8D Engine Jet Noise Reduction. Report No. FAA RD-77-132-1-vol-1 a 2, PWA-5582-vol-1 a 2, Pratt Whitney Aircraft Group, Dec. 1977. (AD-A057309, AD-A05731015).
12. Pond, F. H.; and Heinz, R. A.: JT8D Engine Internal Exhaust Mixer Technology Program. Report No. FAA RD-80-69, PWA-5584-33, Pratt and Whitney Aircraft Group, Apr. 1980. (AD-A093057).
13. Howes, W. L.: Ground Reflection of Jet Noise. NASA TR R-35, 1959.
14. Shields, F. D.; and Bass, H. E.: Atmospheric Absorption of High Frequency Noise and Application to Fractional-Octave Bands. NASA CR-2760, Kime 1977.

15. Gliebe, P. R.; Sandusky, G. T.; and Chamberlin, R.: Mixer Nozzle Aeroacoustic Characteristics for the Energy Efficient Engine. AIAA Paper 81-1994, Oct. 1981.
16. Stone, J. R.; Groesbeck, D. E.; and Zola, C. L.: An Improved Prediction Method for Noise Generated by Conventional Profile Coaxial Jets. AIAA Paper 81-1991, Oct. 1981.
17. Goodykoontz, J. H.; and Stone, J. R.: Experimental Study of Coaxial Nozzle Exhaust Noise. AIAA Paper 79-0631, Mar. 1979.

TABLE I. - NOZZLE FLOW CONDITIONS FOR ACOUSTIC TESTS.

Configuration	Fan stream			Core stream			Ideal nozzle exhaust velocity, m/sec		By-pass ratio, $W_F/W_C$	+Ideal mixed velocity $V_M$ , m/sec
	Pressure ratio, $PR_F$	Total temperature, $T_F$ °K	Flow rate, $w_F$ , kg/sec	Pressure ratio, $PR_C$	Total temperature, $T_C$ °K	Flow rate, $w_C$ , kg/sec	Fan stream, $V_F$ , m/sec	Core stream, $V_C$ , m/sec		
1	1.60	288	5.71	1.60	720	1.43	270	428	3.99	302
3	1.60	297	6.00	1.60	743	1.05	274	435	5.71	298
5	1.60	296	5.93	1.60	737	1.13	274	433	5.25	299
6	1.60	286	5.48	1.60	717	1.54	269	427	3.56	304
8	1.60	289	5.93	1.60	728	1.24	271	430	4.78	296
9	1.59	290	5.98	1.59	726	1.13	269	427	5.29	294
10	1.60	288	5.69	1.60	720	1.41	270	428	4.03	301

$$+ V_M = \frac{W_F V_F + W_C V_C}{W_F + W_C}$$

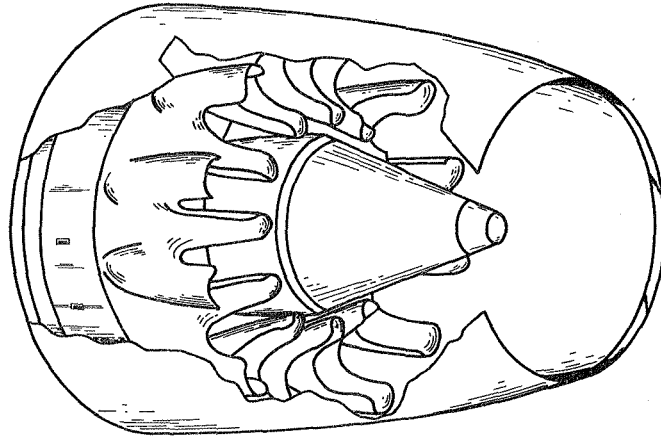


Figure 1. - Schematic of internal lobed mixer nozzle design.

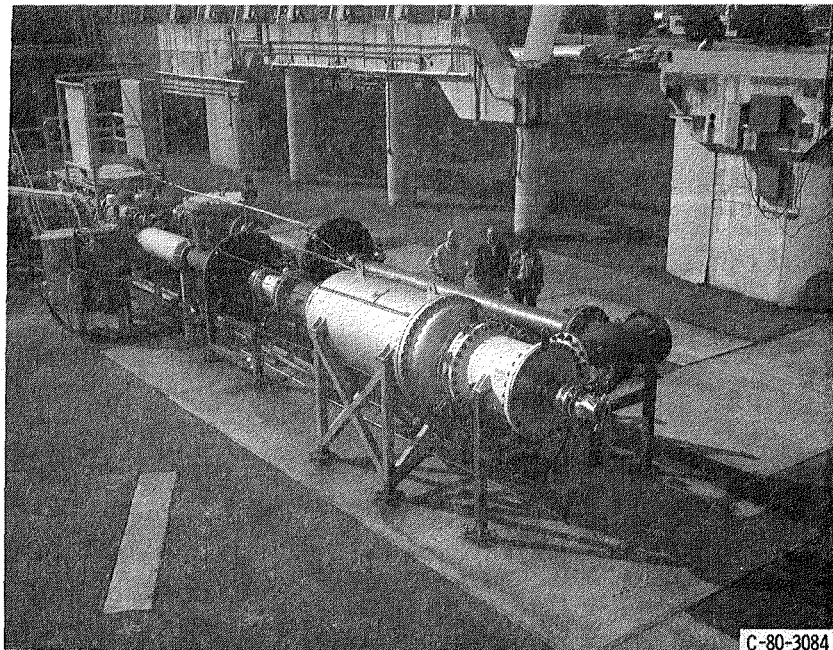
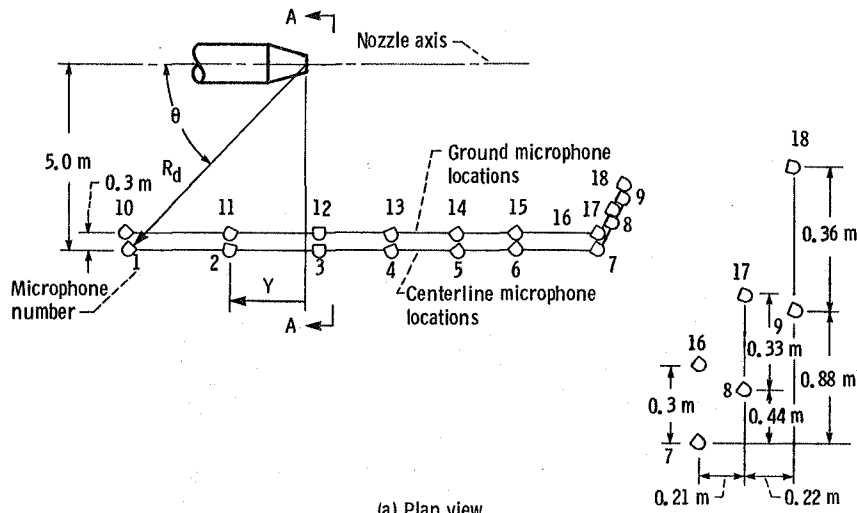


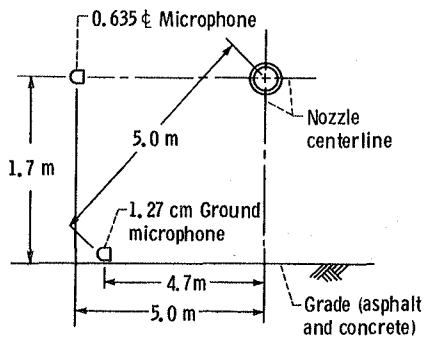
Figure 2. - Internal mixer nozzle test facility.

Microphone number	$\theta$ , deg	$R_d$ , m	$Y$ , m	Effective jet noise angle
1-10	46	6.93	4.84	45
2-11	68	5.39	2.02	65
3-12	95	5.02	-.44	90
4-13	115	5.51	-2.33	110
5-14	129	6.48	-4.04	125
6-15	139	7.60	-5.75	135
7-16	148	9.39	-7.96	145
8-17	151	9.39	-8.21	150
9-18	154	9.39	-8.43	153

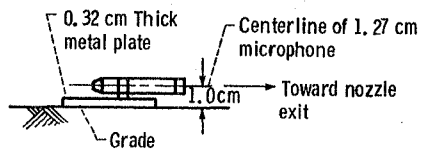


(a) Plan view.

Figure 3. - Microphone layout.



(b) Elevation view A-A



(c) Ground microphone installation detail.

Figure 3. - Concluded.

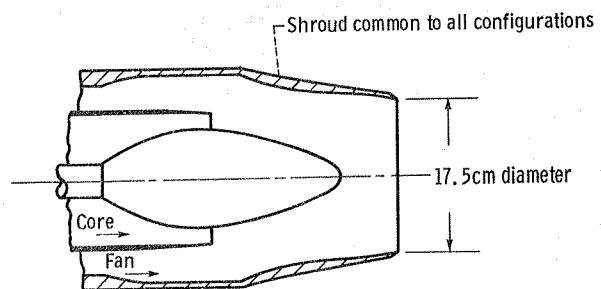


Figure 4. - Schematic of reference annular plug core nozzle configuration. Configuration number 1.

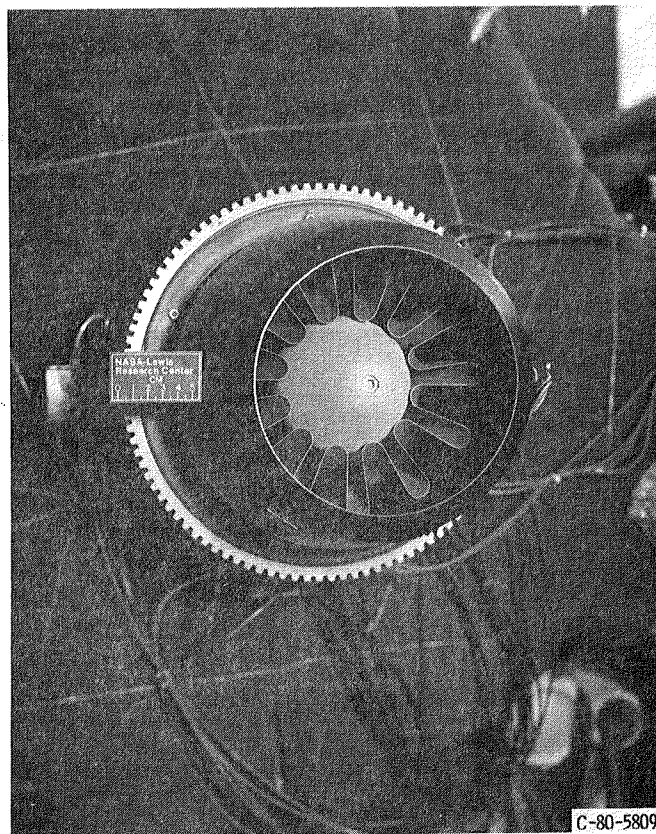


Figure 5. - Typical internal lobed mixer nozzle. (Configuration 3).

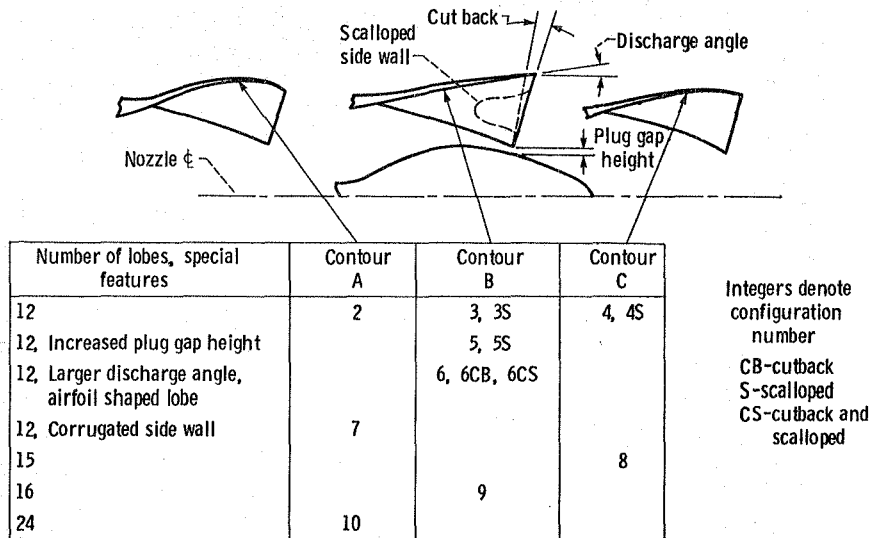


Figure 6. - Summary of lobed internal mixer nozzle configurations.

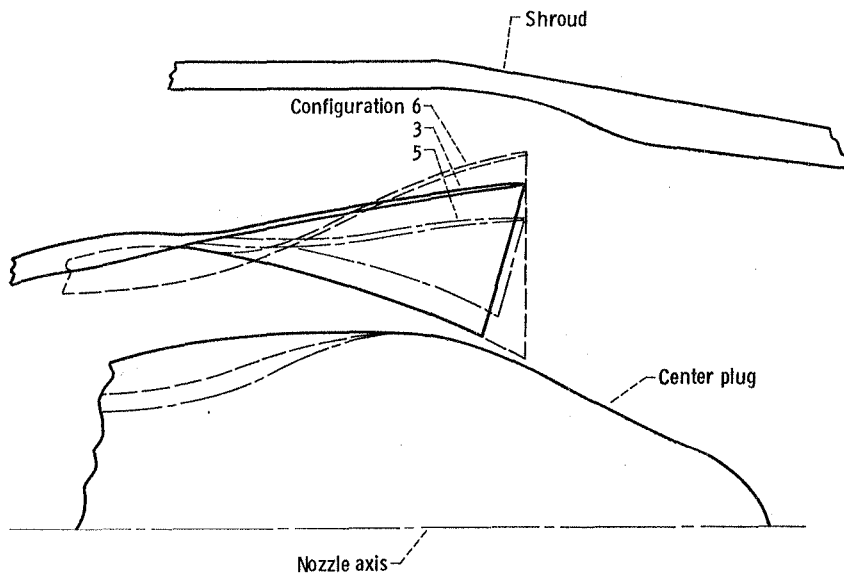


Figure 7. - Detail of lobe design for three mixer nozzle configurations. Twelve lobes, contour B.

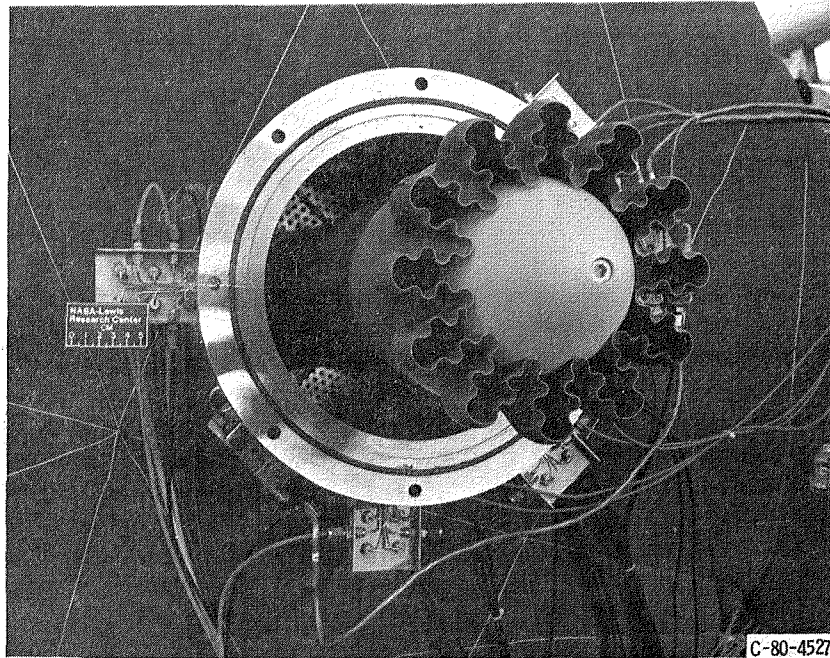


Figure 8. - Corrugated wall mixer nozzle, (Configuration 7).

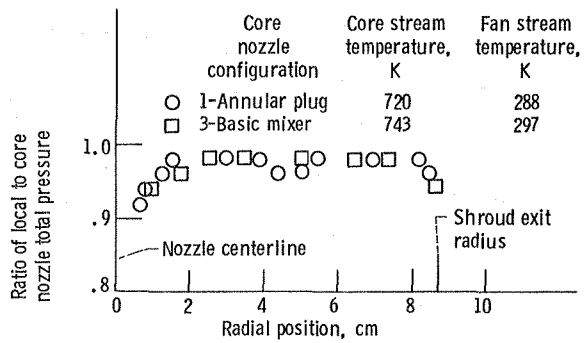


Figure 9. - Variation of total pressure across shroud exit plane.  $PR_F = PR_C = 1.6$ .

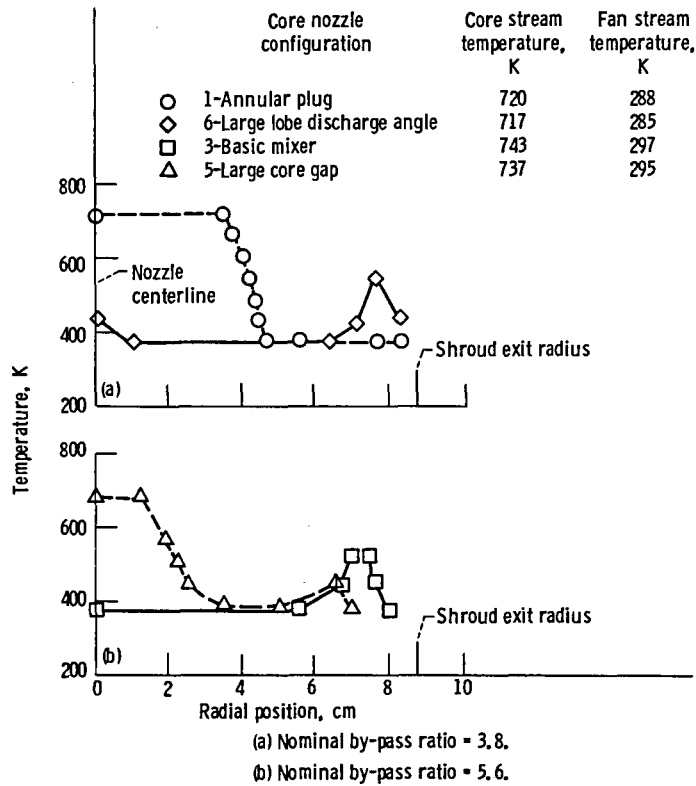


Figure 10. - Total temperature profiles at shroud exit. Measurements for lobed mixer nozzles made downstream of lobe centerline.  $PR_F = PR_C = 1.6$ .

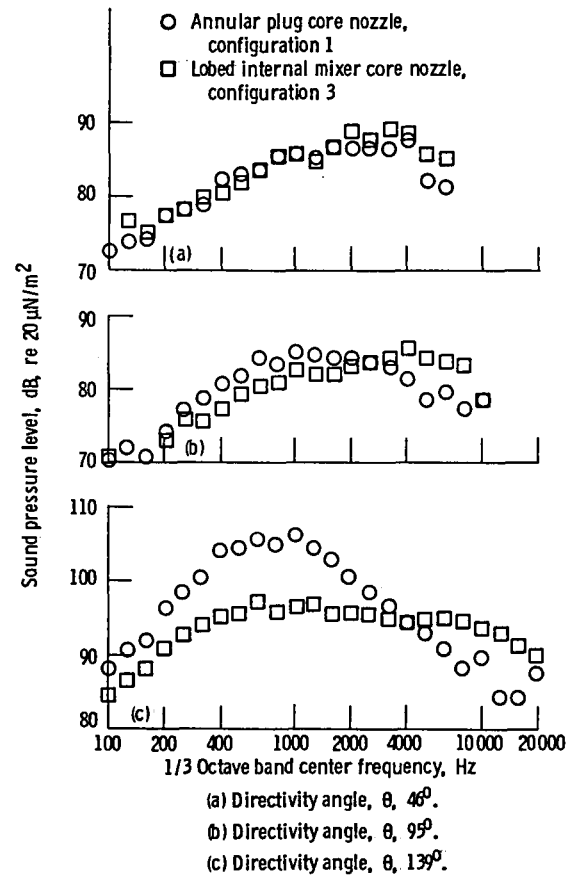


Figure 11. - Comparison of spectral data for annular plug core nozzle and lobed internal mixer core nozzle. Nozzle pressure ratio, 1.6. Nominal temperatures,  $T_C = 732$  K,  $T_F = 243$  K.

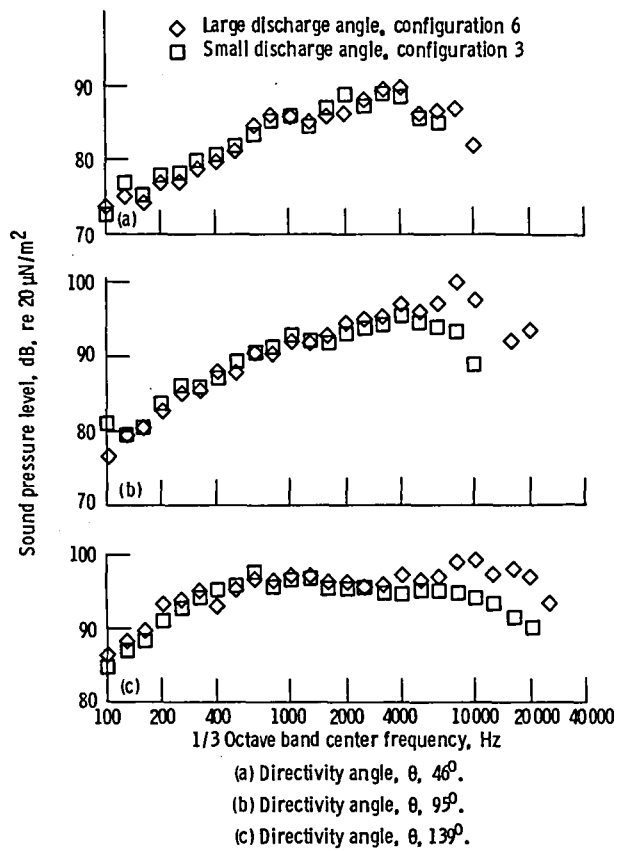


Figure 12. - Effect of variation in lobe discharge angle on sound pressure level spectra for the lobed internal mixer nozzle. Nominal pressure ratio = 1.6. Nominal temperatures  $T_C = 732$  K,  $T_F = 293$  K.

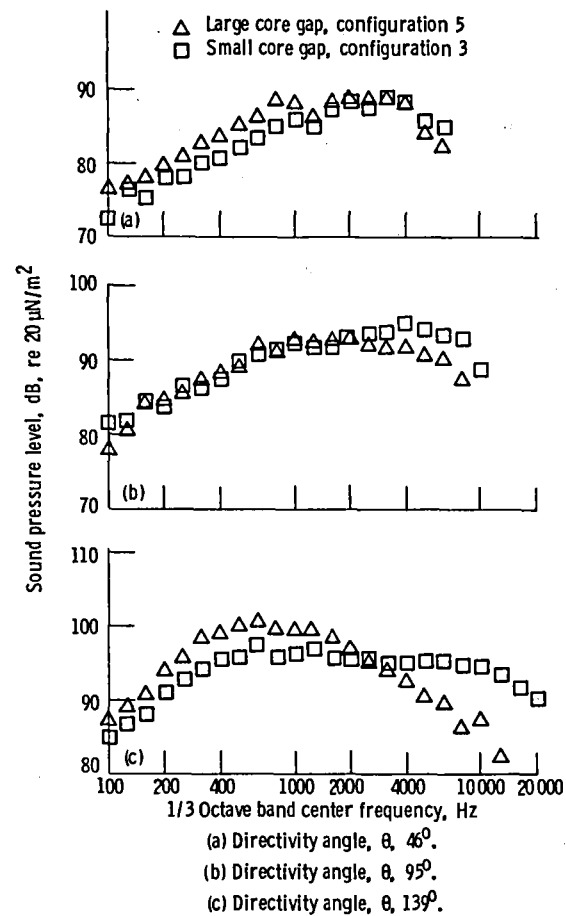


Figure 13. - Effect of variation in plug gap height on sound pressure level spectra for the lobed internal mixer nozzle. Nominal pressure ratio 1.6. Nominal temperatures  $T_C = 732$  K,  $T_F = 293$  K.

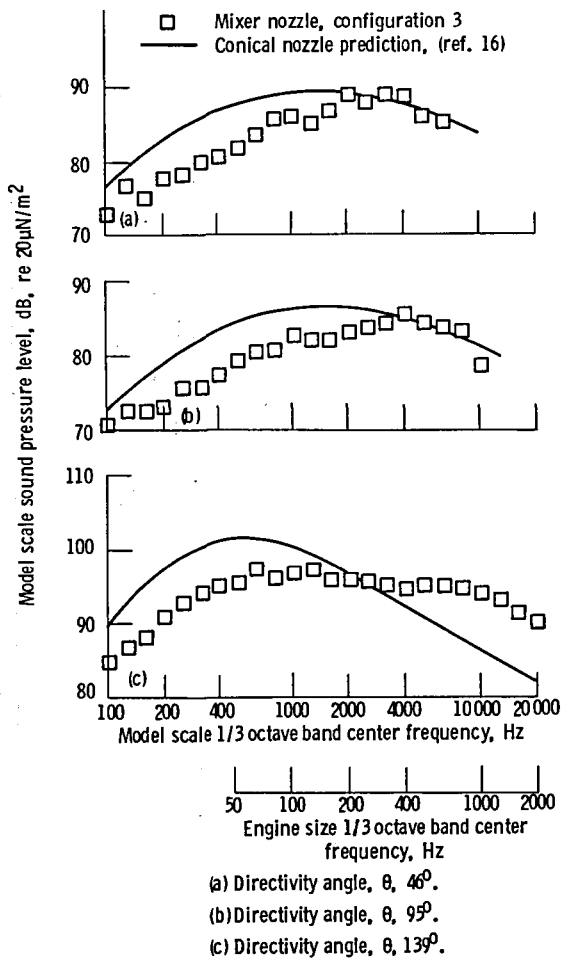


Figure 14. - Comparison of sound pressure level spectra for a lobed internal mixer nozzle and predicted spectra for a conical nozzle. Both nozzles operating at the same value of ideal thrust.  $PR = 1.6$ ,  $V_m = 298$  m/sec,  $T_m = 363$  K,  $D_{con} = 20.3$  cm (model size).

Core stream			
Pressure ratio, $PR_C$	Temperature, $T_C$ , K	Flow rate, $w_C$ , kg/sec	Velocity, $V_C$ , m/sec
1.36	594	1.33	320
1.40	742	.85	371

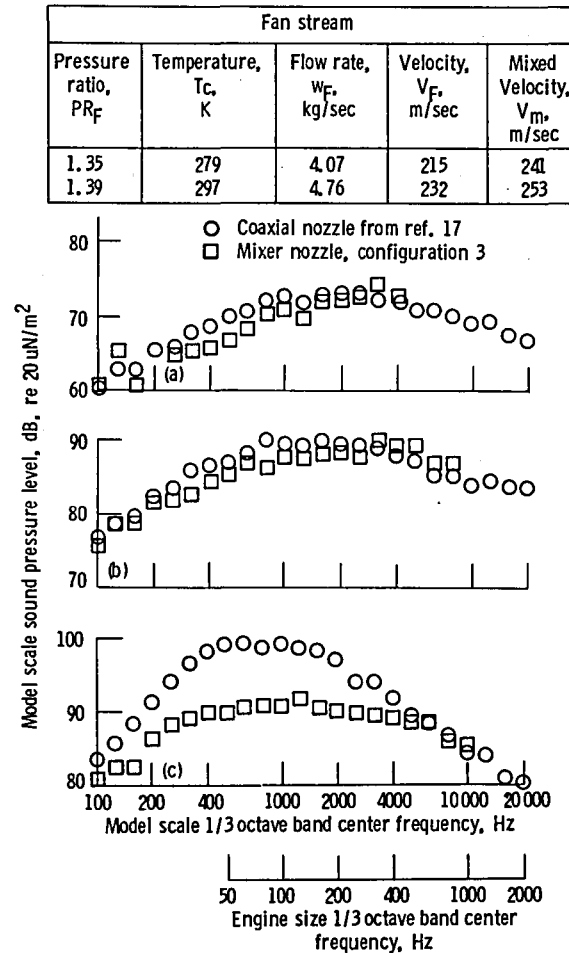


Figure 15. - Comparison of sound pressure level spectra for a lobed internal mixer nozzle and a coaxial nozzle at approximately the same value of ideal thrust. For coaxial nozzle, inner nozzle diameter = 10.0 cm, outer nozzle diameter = 17.6 cm, area ratio = 1.9

Fan stream				
Pressure ratio, $PR_F$	Temperature, $T_C$ , K	Flow rate, $w_F$ , kg/sec	Velocity, $V_F$ , m/sec	Mixed Velocity, $V_m$ , m/sec
1.35	279	4.07	215	241
1.39	297	4.76	232	253

1. Report No. <b>NASA TM-83020</b>	2. Government Accession No.	3. Recipient's Catalog No.	
4. Title and Subtitle <b>EXPERIMENTS ON HIGH BYPASS INTERNAL MIXER NOZZLE JET NOISE</b>		5. Report Date <b>December 1982</b>	
		6. Performing Organization Code <b>505-31-32</b>	
7. Author(s)  <b>Jack H. Goodykoontz</b>		8. Performing Organization Report No. <b>E-1456</b>	
		10. Work Unit No.	
9. Performing Organization Name and Address <b>National Aeronautics and Space Administration Lewis Research Center Cleveland, Ohio 44135</b>		11. Contract or Grant No.	
		13. Type of Report and Period Covered <b>Technical Memorandum</b>	
12. Sponsoring Agency Name and Address <b>National Aeronautics and Space Administration Washington, D. C. 20546</b>		14. Sponsoring Agency Code	
		15. Supplementary Notes	
16. Abstract <p>Model scale jet noise data are presented for a variety of internal lobed mixer nozzle configurations for takeoff power settings in a static environment. The results are presented for a 17.5 cm diameter fan nozzle to show the effect on noise levels caused by changes in geometric shape of the internal, or core flow, nozzle. The geometric variables include the lobe discharge angle, the number of lobes, spacing between the center plug and lobe valley, lobe side wall shape and axial contour of the lobes. An annular plug core flow nozzle was also tested and is used as a baseline for comparative purposes. Comparison of data from the internal lobed configurations showed that the most dominant effect, in terms of the effect on full scale perceived noise levels, was caused by a change in the lobe discharge angle. The results showed that increasing the discharge angle caused an increase as large as 7 dB in sound pressure levels in the high frequency portion of the spectra. Changes in the other geometric variables cause negligible effects.</p>			
17. Key Words (Suggested by Author(s)) <b>Jet noise Mixer nozzles</b>		18. Distribution Statement <b>Unclassified - unlimited STAR Category 71</b>	
19. Security Classif. (of this report) <b>Unclassified</b>	20. Security Classif. (of this page) <b>Unclassified</b>	21. No. of Pages	22. Price*

**End of Document**